

# Imaging X-ray fluorescence spectroscopy using microchannel plate X-ray optics

G.J. Price, G.W. Fraser, J.F. Pearson, I.B. Hutchinson, A.D. Holland, J. Nussey, D. Vernon, D. Pullan and K. Turner

Space Research Centre, Department of Physics and Astronomy, University of Leicester, Leicester LE1 7RH, UK.  
E-mail: gwf@star.le.ac.uk

## Introduction

X-ray fluorescence (XRF) spectroscopy is an important tool for the elemental analysis of all kinds of unknown samples. Almost all laboratory XRF, however, is *non-imaging*, i.e. the fluorescent X-ray spectrum and, hence, the elemental composition, is an average over the illuminated sample area. To obtain elemental maps requires the generation of a small-spot-size X-ray beam, perhaps using a capillary optic and a synchrotron source, and the mechanical scanning of the sample.<sup>1</sup>

For the past three years, funded by an Instrument Development Grant from the UK Engineering and Physical Sciences Research Council (EPSRC), we have been developing a new form of Imaging X-ray Fluorescence Spectrometer (IXRFS). In our design, shown schematically in Figure 1, the sample is uniformly illuminated by a primary X-ray beam and the resulting fluorescent flux focused using a novel microchannel plate (MCP) “relay lens” onto the surface of a Charge Coupled Device (CCD) X-ray detector.<sup>2</sup> Using the spectroscopic capability of the imaging CCD, the IXRFS produces elemental maps with sub-mm spatial resolution but has no moving parts. Both the MCP—a form of capillary optic—and X-ray CCD detector technologies have been developed primarily for applications in X-ray astronomy and planetary science. The IXRFS is in fact “scale invariant”; replacing the lab X-ray source by the solar corona and the lab sample by the surface of an airless, inner solar system body, to give a remote sensing instrument for mapping the surface compositions of the planets.<sup>3</sup>

The proof-of-principle measurements for the IXRFS were made using the Laser Plasma X-ray source at the

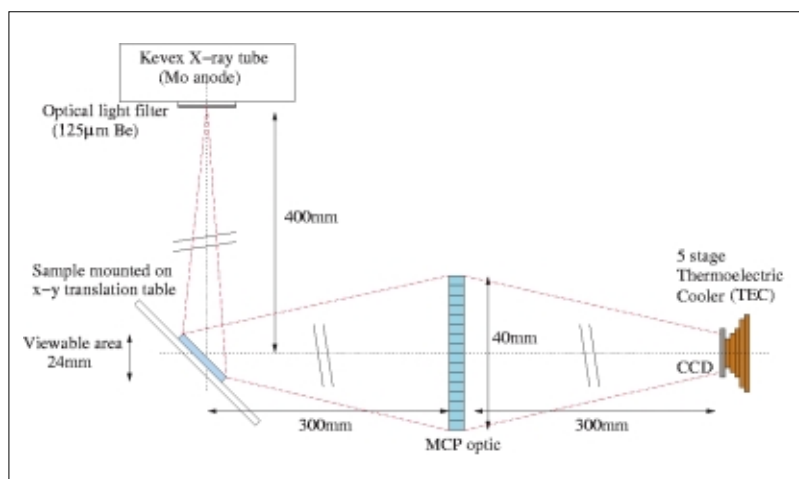


**Figure 1. Schematic of the imaging X-ray fluorescence spectrometer. The magnification of the optic is unity; the instantaneous field of view is therefore the same size as the CCD (24 mm × 24 mm).**

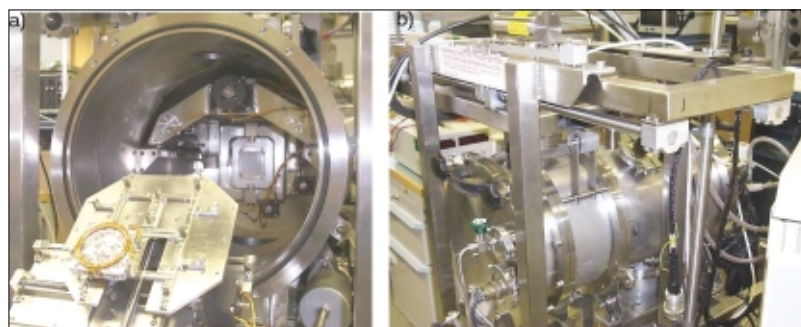


**Figure 2. The IXRFS instrument showing (a) the sample mounting table (with fiducial markers on sample) with the MCP optic in its manipulator (centre of vacuum chamber) and (b) the entire system (the CCD water cooling pipes are visible on the right of the photo; the X-ray tube is in the top left hand corner). The X-ray tube can be run at up to 20 kV and 1 mA emission current.**

CLRC Rutherford Appleton Laboratory in 1997.<sup>2</sup> Further results<sup>4</sup> were obtained in the laboratory at

Leicester before the start of the EPSRC funded programme. Elsewhere, the concept has been extended to higher

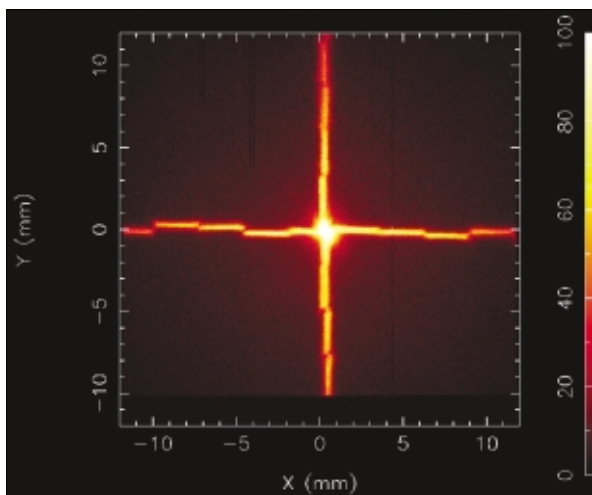


**Figure 3.** The cruxiform point spread function of the planar MCP optic imaged directly using the spectrometer CCD. The FWHM angular resolution is ~7 arcminutes corresponding to a spatial resolution for the system of ~0.7 mm from a FWHM source size of 200  $\mu\text{m}$ .

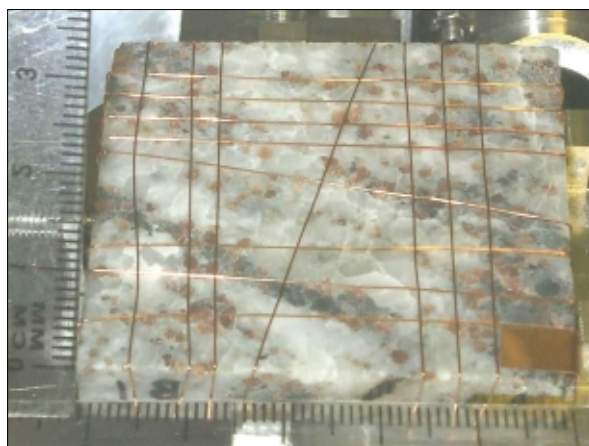


**Figure 4.** Garnetiferous Anorthosite sample wound with wire mesh. The 250  $\mu\text{m}$  diameter copper wires and a piece of copper foil (bottom right) act as fiducial markers for image registration with the X-ray data.

energies at the CHESS synchrotron in the United States.<sup>5</sup>

## Instrument design

The IXRFS instrument, shown in Figures 1 and 2, consists of a commercial electron bombardment X-ray tube (Kevex X-ray, Inc., Scotts Valley, CA, USA) normal to the optical axis of the system, a sample table tilted at 45° to the axis and the MCP optic mounted at the midpoint between the sample and the CCD. The entire system is evacuated to a high vacuum ( $<1 \times 10^{-6}$  mbar) by means of scroll pump backed turbo molecular pumps.

A front illuminated open electrode CCD22 from e2v (e2v technologies, Chelmsford, UK) was selected for the instrument (the same design as the devices on the NASA *Swift* gamma-ray burst experiment and similar to those flown on the XMM-NEWTON X-ray observatory).<sup>6,7</sup> The CCD has 600 by 600 40–40  $\mu\text{m}$  square pixels providing a 24 mm by 24 mm active area. The planar optic has a magnification of unity so this is also the instantaneous field of view of the instrument. The device is cooled via a five-stage Thermo-Electric Cooler (Melcor Corp., Trenton, NJ, USA) providing an operating temperature (using a chilled water supply at ~10°C) of ~-75°C. The CCD has a measured read noise at this temperature of 7–9 electrons giving ~150 eV FWHM energy resolution at 5.9 keV (Mn-K $\alpha$ ). The lower energy limit of the CCD at this temperature is ~370 eV.

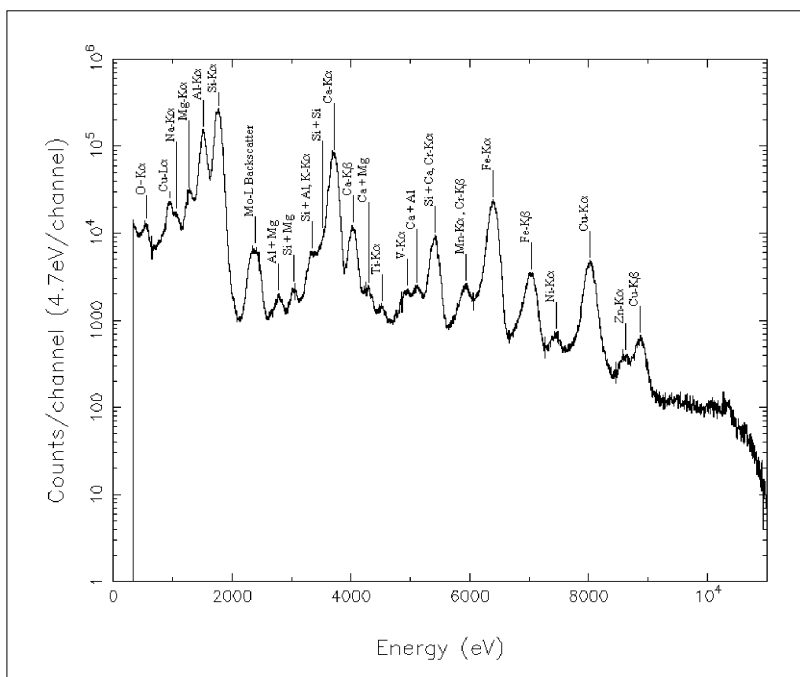


**Figure 5.** CCD spectrum from the sample shown in Figure 4, with peak identification shown vertically.

The MCP optic, manufactured by Photonis (Photonis, Brive, France) from lead silicate glass,<sup>8,9</sup> has 20  $\mu\text{m}$  side length square-pore, square-packed channels on a pitch of 24  $\mu\text{m}$  with an aspect ratio of 50 : 1. The plate is in a planar (point to point focussing) format with an overall area of 40 mm by 40 mm and an open area fraction of ~0.7. The optic is mounted in a two-axis manipulator at the midpoint of the system. By replacing the sample table with the X-ray tube, the cruxiform

point spread function of the optic can be directly measured (Figure 3) and the spectrometer aligned in X-rays. The FWHM (Full Width Half Maximum) angular resolution of the optic is ~7 arcminutes corresponding to a system spatial resolution of ~0.7 mm.

## Results

The CCD software returns an event list containing the position and energy of the imaged X-ray photons on the

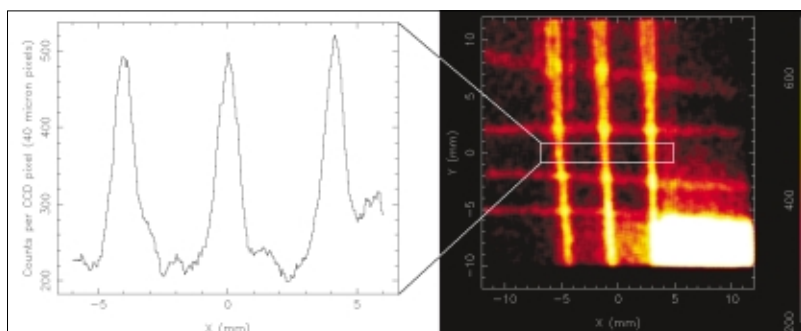


**Figure 6.** X-ray image of the copper wire fiducial markers shown in Figure 4 created from events in the  $\text{Cu-L}_\alpha$  peak in Figure 5. The cut across the image shows a FWHM system resolution of 0.72 mm.

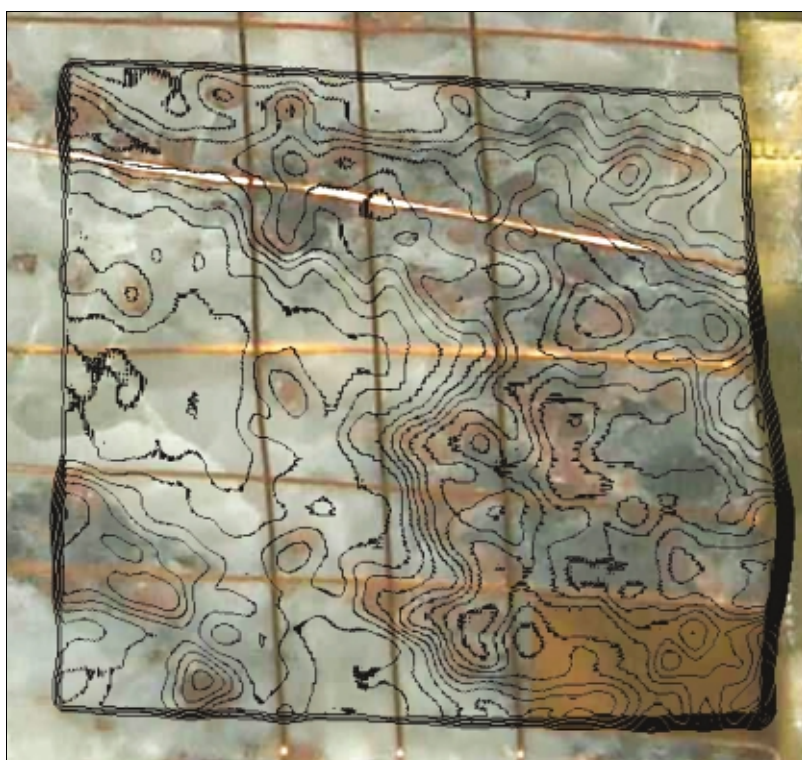


**Figure 7.** Mg/Si contour map overlaid on the sample photograph. The contours run from 0 to 0.25 with a separation of 0.025.

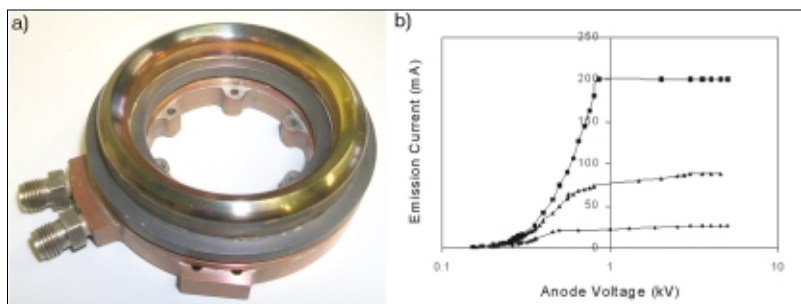


**Figure 8.** (a) Ring anode design. The anode is cooled via the copper block which is electrically insulated from the water by a ceramic spacer. (b) Prototype emission current vs voltage curves for filament currents (bottom to top) of 1.5 A, 1.6 A and 1.7 A, respectively. 200 mA emission current is possible at 1 kV, making high contrast fast imaging below the silicon K edge possible.

device. The spatial origins of spectral peaks on the sample can then be determined and vice versa.

The use of fiducial markers allows the mapping of the CCD X-ray datasets onto photographs of the sample and, hence, correlation of visible features and elemental concentrations. The fiducial markers must be made of a material that isn't expected as a constituent of the sample so that it may be easily identified in the X-ray spectrum. Figure 4 shows a geological sample wound with a fine copper mesh to provide the fiducial marker array.

The corresponding CCD isolated events spectrum is shown in Figure 5. The dataset contains 22 million events, collected in 4900 one-second CCD frames, with a readout time of 8 seconds (0.012 X-rays/pixel/frame). The total integration time was 1 hour 22 minutes over an elapsed time of 12 hours. The X-ray source was run at 10 kV and 1 mA emission current.

The identification of spectral features must take account of (a) scattered X-rays from the primary source, (b) pile up in the CCD pixels (when more than one X-ray is incident in a pixel in a given frame) and (c) escape peaks from the silicon. These features are indicated in Figure 5. Fluorescence from the vacuum system further complicates the spectrum, but the spatial dimension allows these features to be eliminated.

Figure 6 shows the spatial distribution of copper X-rays. The fiducial marker points where the copper wires cross can be clearly seen. A cut through the wires shows the spatial resolution is equal to that of the MCP optic, indicating that the resolution of the optic dominates the system resolution.

Figure 7 shows a map of the Mg/Si ratio superimposed on the sample photo of Figure 4. The dark streaks and brown garnets are magnesium rich in comparison to the background mineral matrix.

An independent mineralogical examination of the sample reveals that the garnets are most likely composed of Almandine and Pyrope ( $\text{Fe}_3\text{Al}_2\text{SiO}_{12}$  and  $\text{Mg}_3\text{Al}_2\text{Si}_3\text{O}_{12}$ , respectively) with the pale remainder made up of a combination of alkaline Feldspars. This confirms the accuracy of the magnesium/silicon ratio map. The Al/Si ratio in common Feldspars ( $\text{XAl}_{(1-2)}\text{Si}_{(3-2)}\text{O}_8$ , where X is an alkaline metal) ranges from 1 to 0.33, this is confirmed in our data.

## Future work

A possible commercial application of the concept described in this article has been the identification of low *Z* surface

contaminants on silicon wafers for the semiconductor industry. Figure 4 shows that it is presently possible to identify elements as far down the periodic table as oxygen, although with a lower noise CCD this could be improved to see the carbon K line.<sup>7</sup>

The main problem with imaging small concentrations of low  $Z$  elements on a silicon wafer is the lack of contrast; the low energy "tail" of the Si-K fluorescence line overwhelms the weaker contaminant signal if the X-ray tube's accelerating voltage is greater than 1.84 kV (Si K edge). In conventional X-ray sources, when the accelerating voltage is turned down, the emission current drops significantly. A new X-ray source is under development at Leicester with an annular geometry. Figure 8 shows the anode design together with an emission current vs voltage curve from a prototype. The filament is suspended just above and outside the annular anode (the large diameter corresponding to ~30 cm of filament) with the sample above it in the centre. The MCP optic and CCD are behind the anode with the secondary flux from the sample transmitted through the hole at its centre.

## Conclusions

A new X-ray fluorescence spectrometer concept has been developed to the point that it is a useful laboratory tool in the non-destructive investigation of sample compositions. When the new low-energy, high-power ring anode comes on line it will be possible to directly image low  $Z$  elements ( $Z$  is the atomic number) on various materials at high contrast with low exposure times. Together with the new generation of high resolution MCP optics under development for an array of X-ray astronomy and planetary missions, a powerful new tool will be available for laboratory analysis.

## Acknowledgements

The authors wish to thank Rob Sareen (Gresham Scientific Instruments, Marlow, UK) for his support. This work was funded by EPSRC Grant No. GR/M51550/01.

## References

1. A commercial system is the EDAX (Kennewick, WA 99336, USA) microprobe, described in B. Scruggs, M. Haschke and P. Pfanekuck, *Adv. X-ray Analysis* **42**, 19 (2000).
2. A.P. Martin, A.N. Brunton, G.W. Fraser, A.D. Holland, A. Keay, J. Hill, N. Nelms, I.C.E. Turcu, R. Allott, N. Lisi and N. Spencer, *X-ray Spectrometry* **28**, 64 (1999).
3. A.P. Martin, A.N. Brunton and G.W. Fraser, *Nucl. Instr. Meth. A* **422**, 567 (1999).
4. A.P. Martin, A.N. Brunton, G.W. Fraser and A.F. Abbey, *Nucl. Instr. Meth. A* **460**, 316 (2001).
5. M. Skala, "Imaging X-ray Fluorescence using microchannel plate (MCP) optics", CHESS report (2000), see <http://www.lns.cornell.edu/public/reu/2000reports/skala.pdf>.
6. M.J.L. Turner *et al.*, *Astronomy and Astrophysics* **365**, L27 (2001).
7. A.D. Short, R.M. Ambrosi, M.J.L. Turner, *Nucl. Instr. Meth. A* **484**, 211 (2002).
8. A.N. Brunton, G.W. Fraser, J.E. Lees and I.C.E. Turcu, *Appl. Opt.* **36**, 5461 (1997).
9. G.J. Price *et al.*, *Nucl. Instr. Meth. A* **490**, 290 (2002).